JACS
JOURNAL OF THE AMERICAN CHEMICAL SOCIETY

Communication

pubs.acs.org/JACS

Side-Chain Effects on the Conductivity, Morphology, and Thermoelectric Properties of Self-Doped Narrow-Band-Gap Conjugated Polyelectrolytes

Cheng-Kang Mai,[†,#,∇] Ruth A. Schlitz,[§,#] Gregory M. Su,[§,#] Daniel Spitzer,[†,∇] Xiaojia Wang,[⊥] Stephanie L. Fronk,[†,∇] David G. Cahill,[⊥] Michael L. Chabinyc,*[,§,#] and Guillermo C. Bazan*[,†,§,#,∇]

[†]Department of Chemistry and Biochemistry, [§]Materials Department, [#]Materials Research Laboratory, and [∇]Center for Polymers and Organic Solids, University of California, Santa Barbara, California 93106, United States

[⊥]Department of Materials Science and Engineering, and Materials Research Laboratory, University of Illinois, Urbana, Illinois 61801, United States

Supporting Information

ABSTRACT: This contribution reports a series of anionic narrow-band-gap self-doped conjugated polyelectrolytes (CPEs) with π-conjugated cyclopenta-[2,1-*b*;3,4-*b*′]-dithiophene-*alt*-4,7-(2,1,3-benzothiadiazole) backbones, but with different counterions (Na^+, K^+, vs tetrabutylammonium) and lengths of alkyl chains (C4 vs C3). These materials were doped to provide air-stable, water-soluble conductive materials. Solid-state electrical conductivity, thermopower, and thermal conductivity were measured and compared. CPEs with smaller counterions and shorter side chains exhibit higher doping levels and form more ordered films. The smallest countercation (Na^+) provides thin films with higher electrical conductivity, but a comparable thermopower, compared to those with larger counterions, thereby leading to a higher power factor. Chemical modifications of the pendant side chains do not influence out of plane thermal conductivity. These studies introduce a novel approach to understand thermoelectric performance by structural modifications.

The majority of thermoelectric materials under investigation are inorganic semiconductors;[1] inorganic/organic composites have also been studied.[2] Organic materials have recently drawn increased attention[3] due to their unique properties, such as low thermal conductivity,[4] synthetic and structural variability, and ease of processing. Thermoelectric efficiency is determined by the dimensionless figure of merit $ZT = S^2\sigma T/\kappa$, where S is the Seebeck coefficient (thermopower), σ the electrical conductivity, κ the thermal conductivity, and T the absolute temperature. Doping of organic semiconductors is commonly used to increase σ for device applications.[5] Both S and σ, and thus the power factor ($PF = S^2\sigma$), have been studied on a variety of conjugated polymers[6] and small molecules.[7]

Self-doped conductive polymers are conjugated polymers in which a significant fraction of monomer units contain covalently attached ionizable functional groups that may act as stable/immobile dopant counterions.[8] Because of the locally available charge-compensating ions, self-doped conductive polymers are interesting candidates for thermoelectric materials. Moreover, an anionic narrow-band-gap conjugated polyelectrolyte, **CPE-K** (Figure 1), was recently reported that can be doped during dialysis to provide a self-doped, water-soluble, and stable conductive polymer.[9] This polymer can serve as a hole-transporting layer in organic solar cells with performance equal to or better than that of PEDOT:PSS (poly(3,4-ethylenedioxythiophene): polystyrenesulfonate).[10] Organic materials with this combination of properties have not been previously examined within the context of thermoelectrics and may provide better-defined systems relative to the much more widely studied PEDOT:PSS.[11]

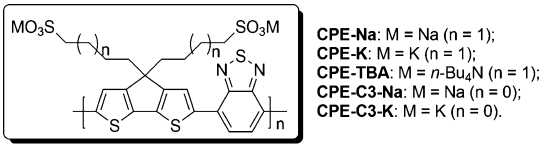

CPE-Na: M = Na (n = 1);
CPE-K: M = K (n = 1);
CPE-TBA: M = *n*-Bu_4N (n = 1);
CPE-C3-Na: M = Na (n = 0);
CPE-C3-K: M = K (n = 0).

Figure 1. Chemical structures of CPEs studied.

Here we report a series of anionic narrow-band-gap conjugated polyelectrolytes (CPEs) with π-conjugated cyclopenta-[2,1-*b*;3,4-*b*′]-dithiophene-*alt*-4,7-(2,1,3-benzothiadiazole) (CPDT-*alt*-BT) backbones, but with different counterions and lengths of alkyl side chains.[9,12] The structures of these materials, namely **CPE-Na**, **CPE-K**, **CPE-TBA**, **CPE-C3-Na**, and **CPE-C3-K**, are shown in Figure 1. Similar *alternating* donor/acceptor units along the backbones of neutral polymers have proven beneficial for achieving high charge mobility in field effect transistors.[13] By measuring their thermoelectric properties along with doping efficiency and morphology, determined by absorption and X-ray scattering, respectively, we can probe the effects of the counterions and alkyl chain length on the thermoelectric performance of these CPEs.

All the CPEs in this study were synthesized via Suzuki–Miyaura polymerization reactions (see Supporting Information, SI) and found to be doped after purification by dialysis.[9] As shown in Figure 2, the UV/vis/NIR absorptions of the CPE thin films on glass substrates confirm their doped nature. They exhibit similar absorption profiles, but with different absorption maxima. The two absorption bands at wavelengths <1000 nm are

Received: April 29, 2014
Published: September 2, 2014

   dx.doi.org/10.1021/ja504284r | *J. Am. Chem. Soc.* 2014, 136, 13478–13481

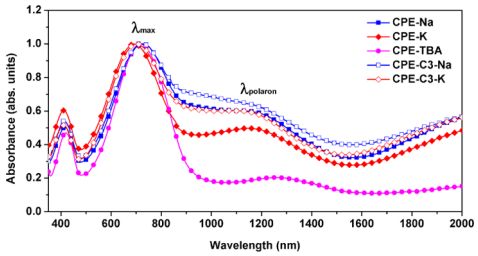

Figure 2. Thin-film absorptions, normalized to λ_{max}, of CPEs on glass substrates. Film thickness (t) and root-mean-square (rms) surface roughness (surface area = 2 μm × 2 μm): **CPE-Na**, t = 32 nm, rms = 640 pm; **CPE-K**, t = 198 nm, rms = 510 pm; **CPE-TBA**, t = 31 nm, rms = 310 pm; **CPE-C3-Na**, t = 78 nm, rms = 860 pm; and **CPE-C3-K**, t = 89 nm, rms = 550 pm.

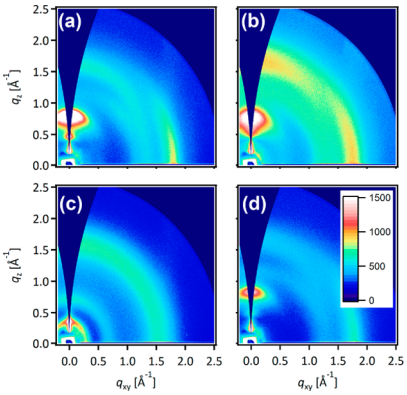

Figure 3. Two-dimensional GIWAXS patterns of thin films on silicon substrates: (a) **CPE-Na**, (b) **CPE-K**, (c) **CPE-TBA**, and (d) **CPE-C3-K**. The color scale shown in panel (d), which corresponds to the scattered intensities (a.u.), applies to all four images.

characteristic of undoped polymers with a CPDT-*alt*-BT backbone.[14] The bands centered around 1250 nm and extending from 1500 nm to >2000 nm most reasonably originate from polaronic transitions ($\lambda_{polaron}$).[11d,15]

The counterions influence the optical properties and extent of doping. In Figure 2, **CPE-Na**, **CPE-K**, and **CPE-TBA**, all of which contain a four-carbon pendant group, exhibit different relative intensity ratios ($\lambda_{polaron}/\lambda_{max}$), probably due to varying doping levels induced by the different counterions. **CPE-Na**, with the smallest counterion, shows the highest $\lambda_{polaron}/\lambda_{max}$, with $\lambda_{polaron}$ located at the lowest wavelength (1084 nm). However, **CPE-Na**, **CPE-K**, and **CPE-TBA** exhibit nearly identical absorption profiles in basic solution (0.1 M KOH), in which these CPEs can be de-doped (see SI, Figure S4b), consistent with the fact that they have the same backbone and similar molecular weights. Finally, it is worth noting that variations of the CPE structures discussed with pendant *cationic* groups show no evidence of doping under the experimental conditions described here.[9]

The length of the alkyl side chain also influences the optical properties. Compared to **CPE-K**, **CPE-C3-K** possesses a greater $\lambda_{polaron}/\lambda_{max}$, implying possibly a higher doping level under similar conditions. This observation also holds true for the comparisons of **CPE-Na** and **CPE-C3-Na**. One plausible explanation is that the shorter side chain brings the negatively charged SO_3^- closer to the conjugated backbone, more readily stabilizing positive charges on the backbone by electrostatic interactions. This proposed explanation is consistent with reports in the literature that self-doped poly-*n*-(3′-thienyl)-alkanesulfonic acids with shorter side chains have higher doping levels due to more effective Coulomb stabilization.[16]

As confirmed by atomic force microscopy (AFM), all the CPEs form smooth films when spun-cast on pre-cleaned glass substrates from the respective solutions (10 mg/mL in 1:1 H_2O:MeOH) using standard spin-coating conditions (see SI). These processing conditions were also used for preparing samples for measurements of σ and S. The choice of counterions impacts the film thickness (t) in a non-obvious way despite identical spin-coating conditions (**CPE-Na**, t = 32 nm; **CPE-K**, t = 198 nm; **CPE-TBA**, t = 31 nm; **CPE-C3-Na**, t = 78 nm; and **CPE-C3-K**, t = 89 nm). All the films are smooth, with root-mean-square (rms) roughness (surface area = 2 μm × 2 μm) of <1 nm. CPEs with larger counterions show slightly smaller rms roughness (**CPE-Na**, rms = 640 pm; **CPE-K**, rms = 510 pm; **CPE-TBA**, rms = 310 pm; **CPE-C3-Na**, rms = 860 pm; and **CPE-C3-K**, rms = 550 pm).

The molecular packing of the films was examined by using grazing incidence wide-angle X-ray scattering (GIWAXS).[17] To the best of our knowledge, the molecular ordering of CPE solids have not been studied by GIWAXS before. It has been previously proposed that a cationic CPE with smaller counteranions exhibits higher charge mobility due to tighter interchain packing distances.[18] As shown in Figure 3, **CPE-Na** and **CPE-K** show similar GIWAXS scattering patterns. The presence of scattering peaks near the q_z axis and the absence of off-axis peaks expected for hexagonal packing, commonly observed in some poly(fluorenes), suggest a layered packing structure for these CPEs.[19] Additionally, a peak at $q_{xy} \approx 1.8$ Å^{-1} corresponds to a relatively tight intermolecular $\pi-\pi$ stacking distance. The in-plane (along q_{xy}) stacking distance for **CPE-Na** (q_{xy} = 1.79 Å^{-1}, d = 3.50 Å) is smaller than that of **CPE-K** (q_{xy} = 1.76 Å^{-1}, d = 3.57 Å). The $\pi-\pi$ stacking distances of these two CPEs are shorter than neutral polymers with the same CPDT-*alt*-BT backbone and linear alkyl side chains (3.7−3.8 Å).[13a] Furthermore, the full width at half-maximum (fwhm) of this peak can be correlated to a crystallite correlation length (CCL) via the Scherrer equation.[17c] The CCL is slightly larger in the **CPE-Na** film (fwhm = 0.24 Å^{-1}, CCL = 2.6 nm), relative to **CPE-K** (fwhm = 0.39 Å^{-1}, CCL = 1.6 nm), indicating larger or more perfect crystallites. In contrast, the scattering pattern of **CPE-TBA** in Figure 3c is more diffuse than those of **CPE-K** or **CPE-Na**, without a clear stacking reflection, suggesting lower crystallinity. Thus, we conclude that the much larger and miscible tetrabutylammonium (TBA) counterions impede crystallization of the polymer chains. Finally, **CPE-C3-K** has a $\pi-\pi$ stacking distance (q_{xy} = 1.77 Å^{-1}, d = 3.54 Å) similar to that of **CPE-K**, but it is more crystalline, as proved by the sharper $\pi-\pi$ stacking peak (fwhm = 0.32 Å^{-1}, CCL = 2.0 nm).

The length of the CPE side chains also modulates the morphology of the films. Figure 4 provides a plot of the intensity distribution for the $\pi-\pi$ stacking reflections of **CPE-K** and **CPE-C3-K** as a function of the polar angle. Polar angles of 0° and 180° correspond to in-plane scattering, and 90° corresponds to out-of-plane scattering. The data in Figure 4 suggest differing crystallite orientations. Compared to **CPE-K**, **CPE-C3-K** has a greater intensity along the in-plane directions (0° and 180°) than the nearly out-of-plane direction (90°).[20] Domain boundaries between edge-on and face-on domains are known to impede charge transport, suggesting that the more even bimodal distribution in **CPE-K** inhibits transport relative to the more dominantly edge-on **CPE-C3-K**.

dx.doi.org/10.1021/ja504284r | J. Am. Chem. Soc. 2014, 136, 13478−13481

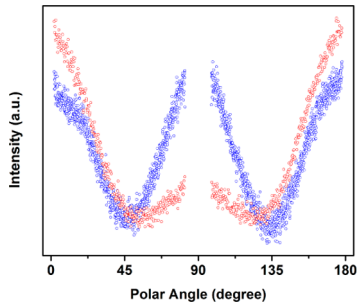

Figure 4. Intensity distribution for the $\pi-\pi$ stacking reflections of **CPE-K** (blue) and **CPE-C3-K** (red). Polar angles of 0° and 180° correspond to in-plane scattering, and 90° corresponds to out-of-plane scattering.

The three thermoelectric properties (S, σ, and κ) of CPE thin films were measured and compared. CPE solutions were spun-cast onto pre-cleaned glass substrates, followed by thermal evaporation of gold electrodes (100 nm) through a mask. S was determined by linear fitting of a data series taken by imposing a temperature difference across the sample and measuring the thermovoltages ($S = -\Delta V/\Delta T$). Thermocouples were attached to the sample via a spring force from the probe arm, and good thermal contact was made with thermal paste. The system was validated by measuring samples of bismuth telluride, silicon, and indium tin oxide, and the uncertainty was determined to be ±10−15%. σ was measured on the same substrate via four-point probe measurements. κ of the thin film spun-cast on silicon substrates was measured along the vertical direction of the film surface employing time-domain thermoreflectance (TDTR).[21] The thermoelectric parameters are summarized, together with PF results, in Table 1.

Table 1. Summary of Thermoelectric Parameters of CPEs

	σ, S/cm	S, μV/K	σS^2, μW/(m·K^2)	κ, W/(m·K)
CPE-Na	0.16 ± 0.005	165 ± 12	0.44	0.26
CPE-K	0.024 ± 0.001	230 ± 10	0.13	0.23
CPE-C4-TBA				0.22
CPE-C3-Na	0.22 ± 0.02	195 ± 5	0.84	–[a]
CPE-C3-K	0.048 ± 0.004	200 ± 18	0.19	0.27

[a]Not measured.

Table 1 reveals that the choice of countercation and alkyl chain length has a clear impact on σ. CPEs with smaller counterions are more conductive than those with larger ones. Specifically, **CPE-Na** (0.16 ± 0.005 S/cm) and **CPE-C3-Na** (0.22 ± 0.02 S/cm) are more conductive than **CPE-K** (0.024 ± 0.001 S/cm) and **CPE-C3-K** (0.048 ± 0.004 S/cm). Shortening the side chains (**CPE-Na** vs **CPE-C3-Na**, and **CPE-K** vs **CPE-C3-K**) appears to be beneficial for improving σ within this series of CPEs. This increase in σ occurs at the expense of difficulties in purification. **CPE-TBA**, on the other hand, proved to be too resistive ($\sigma < 10^{-4}$ S/cm) to be measured with our experimental setup. We note that σ is determined by the charge carrier concentration and mobility.[22] In general, the σ values of these CPEs correlate well with the doping levels, as observed in absorptions (Figure 2). Specifically, higher $\lambda_{polaron}/\lambda_{max}$ leads to higher σ. Moreover, as evidenced in the GIWAXS data (Figure 3), CPEs with higher σ also form more-ordered films, which may contribute to higher carrier mobilities. The low σ of **CPE-TBA** can therefore be attributed to the lowest doping level and the least ordered films.

Conductive organic polymers, like all thermoelectric materials, face a challenge for optimization of the power factors ($S^2\sigma$), due to the inverse relationship between σ and S.[3a,d] The more conductive **CPE-Na** exhibits a lower S (165 ± 12 μV/K) than **CPE-K** (230 ± 10 μV/K). However, the PF of **CPE-Na** (0.44 μW/(m·K^2)) is higher than that of **CPE-K** (0.13 μW/(m·K^2)), due to the higher σ. Similarly, S of the more conductive **CPE-C3-K** (200 ± 18 μV/K) is slightly lower than that of **CPE-K** (230 ± 10 μV/K), and **CPE-C3-K** possesses a higher PF (0.19 μW/(m·K^2)) than **CPE-K** (0.13 μW/(m·K^2)). Interestingly, **CPE-C3-Na** possess σ and S both higher than those of **CPE-Na**, resulting in the highest power factor (0.84 μW/(m·K^2)) among all the CPEs studied.

We further explored the electronic properties of the CPEs using ultraviolet photoemission spectroscopy (UPS). It has been reported that the work function of PEDOT:PSS can be systematically tuned over an eV-wide range by exchanging the excess matrix protons with different counterions.[23] However, in our studies, the work functions of **CPE-Na**, **CPE-K**, and **CPE-C3-K** determined by UPS are almost the same within experimental errors (4.7−4.8 eV). The similar slopes of the UPS data at the Fermi level (see SI) are in agreement with the similar thermopowers of **CPE-Na**, **CPE-K**, and **CPE-C3-K**.[11e]

Thermal annealing of the CPE thin films to 150 °C in a nitrogen-filled glovebox does not lead to substantial differences in σ and S. In general one observes a decrease in σ which is compensated by gains in S (see SI, Table S3). Additionally, AFM shows minor increases in surface roughness (see SI, Figures S6 and S7).

The out-of-plane thermal conductivities of the CPE thin films treated at 80 °C on silicon substrates were measured by the TDTR method, an ultrafast pump/probe laser technique,[21] and found to be almost the same (0.2−0.3 W/(m·K)). These values are within the usual range for neutral conjugated polymers (0.05−0.6 W/(m·K)),[24] which indicates that the ionic content of CPEs does not significantly influence the out-of-plane thermal conductivity. It should be noted that, due to the structural anisotropy of the thin films, it is not appropriate to combine these values and the in-plane electrical transport measurements to obtain ZT. The structural-induced anisotropy of in-plane to out-of-plane thermal conductivities of spin-coated PEDOT was reported to be ∼1.5.[11f] We speculate that the anisotropy of all CPE films should be similar to these literature values.

In conclusion, a new class of water-soluble anionic narrow-band-gap conjugated polyelectrolytes has been designed and synthesized. These materials allow one to gauge thermoelectric properties of easily doped organic semiconductors as a function of counterion and tether length, while keeping the conjugated backbone the same. CPEs with smaller counterions (Na^+, K^+, vs TBA) exhibit higher electrical conductivities with lower thermopowers, most reasonably because of the higher doping efficiency, tighter $\pi-\pi$ stacking, and better crystallinity, as determined by absorption and GIWAXS. Shortening the side chains of CPE leads to increased doping level, better crystallinity, and a more edge-on molecular orientation, all of which provide useful handles to modulate electrical conductivity. Side-chain engineering has been recognized as an effective method to tune the electrical properties of semiconducting conjugated polymers.[25] Our studies highlight the importance of the ionic side chains of CPE to modulate conductivity, morphology, and thermoelectric properties.

dx.doi.org/10.1021/ja504284r | J. Am. Chem. Soc. 2014, 136, 13478−13481

■ ASSOCIATED CONTENT

Supporting Information

Experimental details and characterization data. This material is available free of charge via the Internet at http://pubs.acs.org.

■ AUTHOR INFORMATION

Corresponding Authors

mchabinyc@engineering.ucsb.edu
bazan@chem.ucsb.edu

Notes

The authors declare no competing financial interest.

■ ACKNOWLEDGMENTS

We acknowledge financial support from the AFOSR MURI FA9550-12-1-0002. The MRL Shared Experimental Facilities, AFM, UPS, and GPC, are supported by the MRSEC Program of the NSF under Award No. DMR 1121053; a member of the NSF-funded Materials Research Facilities Network (www.mrfn.org). GIWAXS measurements were carried out at the Stanford Synchrotron Radiation Lightsource, a directorate of SLAC National Accelerator Laboratory and an Office of Science User Facility operated for the U.S. Department of Energy Office of Science by Stanford University. C.-K.M. thanks Dr. Xiaofeng Liu for helpful discussions and proof-reading the manuscript, and Anne Glaudell for help with the thermoelectric measurements.

■ REFERENCES

(1) Snyder, G. J.; Toberer, E. S. *Nat. Mater.* **2008**, *7*, 105−114.

(2) (a) Du, Y.; Shen, S. Z.; Cai, K.; Casey, P. S. *Prog. Polym. Sci.* **2012**, *37*, 820−841. (b) See, K. C.; Feser, J. P.; Chen, C. E.; Majumdar, A.; Urban, J. J.; Segalman, R. A. *Nano Lett.* **2010**, *10*, 4664−4667.

(3) (a) Poehler, T. O.; Katz, H. E. *Energy Environ. Sci.* **2012**, *5*, 8110−8115. (b) Dubey, N.; Leclerc, M. *J. Polym. Sci., Part B: Polym. Phys.* **2011**, *49*, 467−475. (c) Bubnova, O.; Crispin, X. *Energy Environ. Sci.* **2012**, *5*, 9345−9362. (d) Zhang, Q.; Sun, Y.; Xu, W.; Zhu, D. *Adv. Mater.* **2014**, DOI: 10.1002/adma.201305371.

(4) Choy, C. *Polymer* **1977**, *18*, 984−1004.

(5) Kar, P. *Doping in conjugated polymers*; Scrivener Publishing/Wiley: Hoboken, NJ, 2013.

(6) (a) Sun, J.; Yeh, M.-L.; Jung, B. J.; Zhang, B.; Feser, J.; Majumdar, A.; Katz, H. E. *Macromolecules* **2010**, *43*, 2897−2903. (b) Kaiser, A. *Phys. Rev. B* **1989**, *40*, 2806−2813. (c) Mateeva, N.; Niculescu, H.; Schlenoff, J.; Testardi, L. R. *J. Appl. Phys.* **1998**, *83*, 3111. (d) Sun, Y.; Sheng, P.; Di, C.; Jiao, F.; Xu, W.; Qiu, D.; Zhu, D. *Adv. Mater.* **2012**, *24*, 932−937. (e) Zhang, Q.; Sun, Y.; Xu, W.; Zhu, D. *Energy Environ. Sci.* **2012**, *5*, 10−15. (f) Aïch, R. B.; Blouin, N.; Bouchard, A.; Leclerc, M. *Chem. Mater.* **2009**, *21*, 751−757. (g) Lévesque, I.; Bertrand, P.; Blouin, N. *Chem. Mater.* **2007**, 2128−2138. (h) Lévesque, I.; Bertrand, P.-O.; Blouin, N.; Leclerc, M.; Zecchin, S.; Zotti, G.; Ratcliffe, C. I.; Klug, D. D.; Gao, X.; Gao, F.; Tse, J. S. *Chem. Mater.* **2007**, *19*, 2128−2138. (i) Hiroshige, Y.; Ookawa, M.; Toshima, N. *Synth. Met.* **2006**, *156*, 1341−1347. (j) Hiroshige, Y.; Ookawa, M.; Toshima, N. *Synth. Met.* **2007**, *157*, 467−474. (k) Xuan, Y.; Liu, X.; Desbief, S.; Leclère, P.; Fahlman, M.; Lazzaroni, R.; Berggren, M.; Cornil, J.; Emin, D.; Crispin, X. *Phys. Rev. B* **2010**, *82*, 115454−115459. (l) Yue, R.; Chen, S.; Lu, B.; Liu, C.; Xu, J. *J. Solid State Electrochem.* **2010**, *15*, 539−548. (m) Schlitz, R. A.; Brunetti, F. G.; Glaudell, A. M.; Miller, P. L.; Brady, M. A.; Takacs, C. J.; Hawker, C. J.; Chabinyc, M. L. *Adv. Mater.* **2014**, *26*, 2825−2830. (n) Lu, G.; Bu, L.; Li, S.; Yang, X. *Adv. Mater.* **2014**, *26*, 2359−2364.

(7) (a) Russ, B.; Robb, M. J.; Brunetti, F. G.; Miller, P. L.; Perry, E. E.; Patel, S. N.; Ho, V.; Chang, W. B.; Urban, J. J.; Chabinyc, M. L.; Hawker, C. J.; Segalman, R. A. *Adv. Mater.* **2014**, *26*, 3473−3477. (b) Walzer, K.; Maennig, B.; Pfeiffer, M.; Leo, K. *Chem. Rev.* **2007**, *107*, 1233−1271. (c) Menke, T.; Wei, P.; Ray, D.; Kleemann, H.; Naab, B. D.; Bao, Z.; Leo, K.; Riede, M. *Org. Electron.* **2012**, *13*, 3319−3325. (d) Menke, T.; Ray, D.; Kleemann, H.; Hein, M. P.; Leo, K.; Riede, M. *Org. Electron.* **2014**, *15*, 365−371.

(8) (a) Freund, M. S.; Deore, B. A. *Self-Doped Conducting Polymers*; John Wiley & Sons Ltd.: Chichester, England, 2007. (b) Patil, A. O.; Ikenoue, Y.; Wudl, F.; Heeger, A. J. *J. Am. Chem. Soc.* **1987**, *109*, 1858−1859.

(9) Mai, C.-K.; Zhou, H.; Zhang, Y.; Henson, Z. B.; Nguyen, T.-Q.; Heeger, A. J.; Bazan, G. C. *Angew. Chem., Int. Ed.* **2013**, *52*, 12874−12878.

(10) Zhou, H.; Zhang, Y.; Mai, C.-K.; Collins, S. D.; Nguyen, T.-Q.; Bazan, G. C.; Heeger, A. J. *Adv. Mater.* **2014**, *26*, 780−785.

(11) (a) Yue, R.; Xu, J. *Synth. Met.* **2012**, *162*, 912−917. (b) Bubnova, O.; Berggren, M.; Crispin, X. *J. Am. Chem. Soc.* **2012**, *134*, 16456−16459. (c) Park, T.; Park, C.; Kim, B.; Shin, H.; Kim, E. *Energy Environ. Sci.* **2013**, *6*, 788−792. (d) Bubnova, O.; Khan, Z. U.; Malti, A.; Braun, S.; Fahlman, M.; Berggren, M.; Crispin, X. *Nat. Mater.* **2011**, *10*, 429−433. (e) Bubnova, O.; Khan, Z. U.; Wang, H.; Braun, S.; Evans, D. R.; Fabretto, M.; Hojati-Talemi, P.; Dagnelund, D.; Arlin, J.-B.; Geerts, Y. H.; Desbief, S.; Breiby, D. W.; Andreasen, J. W.; Lazzaroni, R.; Chen, W. M.; Zozoulenko, I.; Fahlman, M.; Murphy, P. J.; Berggren, M.; Crispin, X. *Nat. Mater.* **2014**, *13*, 190−194. (f) Kim, G.-H.; Shao, L.; Zhang, K.; Pipe, K. P. *Nat. Mater.* **2013**, *12*, 719−723.

(12) Li, Y.; Mai, C.-K.; Phan, H.; Liu, X.; Nguyen, T.-Q.; Bazan, G. C.; Chan-Park, M. B. *Adv. Mater.* **2014**, *26*, 4697−4703.

(13) (a) Tsao, H. N.; Cho, D. M.; Park, I.; Hansen, M. R.; Mavrinskiy, A.; Yoon, D. Y.; Graf, R.; Pisula, W.; Spiess, H. W.; Müllen, K. *J. Am. Chem. Soc.* **2011**, *133*, 2605−2612. (b) Ying, L.; Hsu, B. B. Y.; Zhan, H.; Welch, G. C.; Zalar, P.; Perez, L. A.; Kramer, E. J.; Nguyen, T.-Q.; Heeger, A. J.; Wong, W.-Y.; Bazan, G. C. *J. Am. Chem. Soc.* **2011**, *133*, 18538−18541. (c) Tseng, H.-R.; Ying, L.; Hsu, B. B. Y.; Perez, L. A.; Takacs, C. J.; Bazan, G. C.; Heeger, A. J. *Nano Lett.* **2012**, *12*, 6353−6357.

(14) (a) Mühlbacher, D.; Scharber, M.; Morana, M.; Zhu, Z.; Waller, D.; Gaudiana, R.; Brabec, C. *Adv. Mater.* **2006**, *18*, 2884−2889. (b) Soci, C.; Hwang, I.-W.; Moses, D.; Zhu, Z.; Waller, D.; Gaudiana, R.; Brabec, C. J.; Heeger, A. J. *Adv. Funct. Mater.* **2007**, *17*, 632−636.

(15) Beaujuge, P. M.; Vasilyeva, S. V.; Ellinger, S.; McCarley, T. D.; Reynolds, J. R. *Macromolecules* **2009**, *42*, 3694−3706.

(16) Chen, S. A.; Hua, M. Y. *Macromolecules* **1993**, *26*, 7108−7110.

(17) (a) Brady, M. A.; Su, G. M.; Chabinyc, M. L. *Soft Matter* **2011**, *7*, 11065−11077. (b) Chen, W.; Nikiforov, M. P.; Darling, S. B. *Energy Environ. Sci.* **2012**, *5*, 8045−8074. (c) Rivnay, J.; Mannsfeld, S. C. B.; Miller, C. E.; Salleo, A.; Toney, M. F. *Chem. Rev.* **2012**, *112*, 5488−5519.

(18) (a) Yang, R.; Garcia, A.; Korystov, D.; Mikhailovsky, A.; Bazan, G. C.; Nguyen, T.-Q. *J. Am. Chem. Soc.* **2006**, *128*, 16532−16539. (b) Yang, R.; Wu, H.; Cao, Y.; Bazan, G. C. *J. Am. Chem. Soc.* **2006**, *128*, 14422−14423.

(19) Knaapila, M.; Lyons, B. P.; Kisko, K.; Foreman, J. P.; Vainio, U.; Mihaylova, M.; Seeck, O. H.; Pålsson, L.-O.; Serimaa, R.; Torkkeli, M.; Monkman, A. P. *J. Phys. Chem. B* **2003**, *107*, 12425−12430.

(20) Osaka, I.; Saito, M.; Koganezawa, T.; Takimiya, K. *Adv. Mater.* **2014**, *26*, 331−338.

(21) (a) Koh, Y.; Cahill, D. *Phys. Rev. B* **2007**, *76*, 075207. (b) Wang, X.; Ho, V.; Segalman, R. A.; Cahill, D. G. *Macromolecules* **2013**, *46*, 4937−4943. (c) Wang, X.; Liman, C. D.; Treat, N. D.; Chabinyc, M. L.; Cahill, D. G. *Phys. Rev. B* **2013**, *88*, 075310.

(22) Kaiser, A. B.; Skákalová, V. *Chem. Soc. Rev.* **2011**, *40*, 3786−3801.

(23) Chia, P.-J.; Sivaramakrishnan, S.; Zhou, M.; Png, R.-Q.; Chua, L.-L.; Friend, R.; Ho, P. *Phys. Rev. Lett.* **2009**, *102*, 096602.

(24) (a) Yan, H.; Ohno, N.; Toshima, N. *Chem. Lett.* **2000**, 392−393. (b) Yan, H.; Sada, N.; Toshima, N. *J. Therm. Anal. Calorim.* **2002**, *69*, 881−887. (c) Kaul, P. B.; Day, K. A.; Abramson, A. R. *J. Appl. Phys.* **2007**, *101*, 083507.

(25) (a) Lei, T.; Wang, J.-Y.; Pei, J. *Chem. Mater.* **2014**, *26*, 594−603. (b) Mei, J.; Bao, Z. *Chem. Mater.* **2013**, *26*, 604−615.